Mobile Manipulation of Flexible Objects Under Deformation Constraints

Herbert G. Tanner, *Member, IEEE*

***Abstract*— We develop a velocity field tracking control scheme with PI force feedback to transport and manipulate deformable material with a mobile manipulator. We assume that the deformable object is a damped underactuated mechanical system. The input-to-state stability properties of its zero dynamics are used to derive bounds on the admissible end-effector velocities and accelerations. It is shown both analytically and in simulation, that using deformation feedback we can avoid exciting excessive object deformations.**

***Index Terms*— Mobile Manipulators, Deformable Objects, Force Control, Nonholonomic Systems**

I. Introduction

To automate the handling of deformable objects, we need detailed object models and control schemes that enable safe manipulation. Existing robot controllers for deformable manipulation typically do not use object state feedback. Their purpose is to eliminate internal forces and vibrations [1], [2], [3], [4]. Similarly, in swing-free manipulation the objective is to eliminate residual oscillation of a suspended object [5], [6]. These methods use an object model [7], [8], [9] in an open loop fashion. The technology to obtain direct feedback from deformable objects advances quickly [10], [11].

In this paper the control objective is not to suppress vibrations, but rather to keep them bounded using object state feedback. Some object deformation may be admissible, and sometimes even desirable [12], to adjust the shape of the system and navigate in cluttered environments. The limits of the control inputs are specified based on the stability properties of the deformable object dynamics. A PI force control loop is closed around the velocity tracking controller, to ensure that forces exerted on the object remain within admissible limits and the effect of model uncertainty is minimized. We develop a velocity tracking control algorithm [13], which steers the robot along the gradient of a navigation function [14], and stabilizes the object to a desired configuration. Based on the velocity error at each state, we define a desired task space acceleration vector. Since mobile manipulators are usually kinematically redundant, and given that dynamic pseudoinverse-based redundancy resolution inevitably introduces instabilities [15], [16] we directly project task space accelerations to joint space accelerations, exploiting the kinematic structure of the robot.

Manuscript first submitted October 26, 2004; first revision January 28, 2005; second revision May 25, 2005.

H. Tanner is with the Mechanical Engineering Department at the University of New Mexico, MSC01 1150, Albuquerque NM 87131-0001, E-mail: tanner@unm.edu.

II. System Dynamics

A. Mobile Manipulator

The mobile manipulator considered is a nonholonomic, kinematically redundant system. Its mobile base is described kinematically by the equations of the unicycle:

$$\dot{x} = u_1 \cos\theta, \qquad \dot{y} = u_1 \sin\theta, \qquad \dot{\theta} = u_2,$$

where (x, y) is the pair of planar position coordinates for the base, θ is its orientation and u_1, u_2 are the translational and rotational velocity, respectively. Let $\boldsymbol{q}_b \triangleq \begin{bmatrix} x & y & \theta \end{bmatrix}^T$ denote the coordinates for the mobile base. If $\boldsymbol{q}_a \in \mathbb{R}^6$ is the vector of joint coordinates of the manipulator attached to the base, then the generalized coordinates and velocity vectors for the mobile manipulator can be expressed as $\boldsymbol{q} \triangleq \begin{bmatrix} \boldsymbol{q}_b^T & \boldsymbol{q}_a^T \end{bmatrix}^T$, and $\boldsymbol{u} \triangleq \begin{bmatrix} u_1 & u_2 & \dot{\boldsymbol{q}}_a^T \end{bmatrix}^T$. The task space velocities are related to the joint velocities through the analytic Jacobian:

$$\dot{\boldsymbol{x}}_a = \mathsf{J}_A \, \boldsymbol{u} \equiv \begin{bmatrix} \mathsf{J}_{Ab} & \mathsf{J}_{Aa} \end{bmatrix} \begin{bmatrix} u_1 & u_2 & \dot{\boldsymbol{q}}_a^T \end{bmatrix}^T. \tag{1}$$

Since the system is kinematically redundant, J_A is non-square and "fat". With external forces and torques, $\boldsymbol{F}$, exerted on the end-effector, the robot dynamics become

$$\mathsf{M}_r(\boldsymbol{q}) \, \dot{\boldsymbol{u}} + \boldsymbol{C}_r(\boldsymbol{q}, \boldsymbol{u}) = \boldsymbol{T}_r - \mathsf{J}_A^T \boldsymbol{F}, \tag{2}$$

where M_r is the inertia matrix of the robot system, $\boldsymbol{C}_r$ denotes the vector of Coriolis, centrifugal and gravity terms, and $\boldsymbol{T}_r$ is the vector of generalized forces. This vector includes the control inputs: the force f_b exerted on the base in the direction of θ, the steering torque α_b and the joint torques $\boldsymbol{\tau}_a$: $\boldsymbol{T}_r \triangleq \begin{bmatrix} f_b & \alpha_b & \boldsymbol{\tau}_a^T \end{bmatrix}^T$. The task space dynamics are:

$$\mathcal{M}(\boldsymbol{q}) \, \ddot{\boldsymbol{x}}_a + \mathcal{C}(\boldsymbol{q}, \boldsymbol{u}) = \mathcal{T} - \boldsymbol{F}, \tag{3}$$

where

$$\begin{aligned} &\mathcal{M} \triangleq (\mathsf{J}_A \mathsf{M}_r^{-1} \mathsf{J}_A^T)^{-1}, \quad \mathcal{C} \triangleq \mathcal{M} \mathsf{J}_A \mathsf{M}_r^{-1} \boldsymbol{C}_r - \mathcal{M} \dot{\mathsf{J}}_A \boldsymbol{u}, \\ &\bar{\mathsf{J}}_A \triangleq \mathsf{M}_r^{-1} \mathsf{J}_A^T \mathcal{M}, \qquad \mathcal{T} \triangleq \bar{\mathsf{J}}_A^T \boldsymbol{T}_t. \end{aligned} \tag{4}$$

B. Deformable Object

The deformable object is considered as an underactuated mechanical system [17]. Its actuated degrees of freedom are the coordinates of the grasp points, assumed to coincide with the end-effector's coordinates. The object is described by two sets of variables: the actuated coordinates, $\boldsymbol{z}_1 \equiv \boldsymbol{x}_a$, and the unactuated coordinates $\boldsymbol{z}_2$, the latter expressing the object's "internal" motion. Define the vector of object generalized coordinates as $\boldsymbol{z} \triangleq [\boldsymbol{z}_1^T \ \boldsymbol{z}_2^T]^T$. Its dynamics are written as:

$$\mathsf{M}_o(\boldsymbol{z}) \ddot{\boldsymbol{z}} + \boldsymbol{C}_o(\boldsymbol{z}, \dot{\boldsymbol{z}}) + \mathsf{D}_o \dot{\boldsymbol{z}} + \mathsf{K}_o \boldsymbol{z} = \boldsymbol{T}_o(\boldsymbol{z}), \tag{5}$$

where M_o is the object's inertia matrix, $\boldsymbol{C}_o$ is the vector of Coriolis, centrifugal and gravity terms, D_o is a positive definite diagonal matrix, and K_o is the object's stiffness matrix. The vector $\boldsymbol{T}_o$ is the generalized force exerted on the object. By rearranging the elements in $\boldsymbol{z}$, we partition (5) as:

$$\mathsf{m}_{o_{11}}\ddot{\boldsymbol{z}}_1 + \mathsf{m}_{o_{12}}\ddot{\boldsymbol{z}}_2 + \boldsymbol{c}_{o_1} + \mathsf{d}_{o_1}\dot{\boldsymbol{z}} + \mathsf{k}_{o_1}\boldsymbol{z} + \boldsymbol{t}_{o_1} = \boldsymbol{f}^o \quad (6a)$$
$$\mathsf{m}_{o_{12}}\ddot{\boldsymbol{z}}_1 + \mathsf{m}_{o_{22}}\ddot{\boldsymbol{z}}_2 + \boldsymbol{c}_{o_2} + \mathsf{d}_{o_2}\dot{\boldsymbol{z}} + \mathsf{k}_{o_2}\boldsymbol{z} + \boldsymbol{t}_{o_2} = \boldsymbol{0} \quad (6b)$$

C. Combined Dynamics

Note that $\boldsymbol{f}^o = \boldsymbol{F}$. Combining (6a)-(6b) with (2):

$$\mathsf{M}_r\,\dot{\boldsymbol{u}} + \boldsymbol{C}_r + \mathsf{J}_A^T[\mathsf{m}_{o_{11}}\,\ddot{\boldsymbol{z}}_1 + \mathsf{m}_{o_{12}}\,\ddot{\boldsymbol{z}}_2 + \boldsymbol{c}_{o_1} + \mathsf{d}_{o_1}\,\dot{\boldsymbol{z}} + \mathsf{k}_{o_1}\boldsymbol{z} + \boldsymbol{t}_{o_1}] = \boldsymbol{T}_r$$
$$\mathsf{m}_{o_{12}}\,\ddot{\boldsymbol{z}}_1 + \mathsf{m}_{o_{22}}\,\ddot{\boldsymbol{z}}_2 + \boldsymbol{c}_{o_2} + \mathsf{d}_{o_2}\,\dot{\boldsymbol{z}} + \mathsf{k}_{o_2}\boldsymbol{z} + \boldsymbol{t}_{o_2} = \boldsymbol{0}.$$

The above can be arranged in the form:

$$\begin{bmatrix}\mathsf{M}_{bb} & \mathsf{M}_{ba} & \mathsf{M}_{bo}\\ \mathsf{M}_{ba}^T & \mathsf{M}_{aa} & \mathsf{M}_{ao}\\ \mathsf{M}_{bo}^T & \mathsf{M}_{ao}^T & \mathsf{M}_{oo}\end{bmatrix}\begin{bmatrix}\ddot{\boldsymbol{q}}_b\\ \ddot{\boldsymbol{q}}_a\\ \ddot{\boldsymbol{z}}_2\end{bmatrix} + \begin{bmatrix}\boldsymbol{C}_{rb}\\ \boldsymbol{C}_{ra}\\ \boldsymbol{C}_o\end{bmatrix} = \begin{bmatrix}\boldsymbol{\tau}_b\\ \boldsymbol{\tau}_a\\ \boldsymbol{0}\end{bmatrix}, \quad (7)$$

renaming $[f_b,\ \alpha_b]^T \triangleq \boldsymbol{\tau}_b$. Using equation (3) the combined actuated task space dynamics become:

$$[\mathcal{M} + \mathsf{m}_{o_{11}} - \mathsf{m}_{o_{12}}(\mathsf{m}_{o_{22}})^{-1}\mathsf{m}_{o_{12}}]\ddot{\boldsymbol{x}}_a + \boldsymbol{N} = \mathcal{T} \quad (8)$$

where $\boldsymbol{N} \triangleq -\mathsf{m}_{o_{12}}(\mathsf{m}_{o_{22}})^{-1}(\boldsymbol{c}_{o_2} + \mathsf{d}_{o_2}\,\dot{\boldsymbol{z}} + \mathsf{k}_{o_2}\boldsymbol{z} + \boldsymbol{t}_{o_2})\mathcal{C} + \boldsymbol{c}_{o_1} + \mathsf{d}_{o_1}\,\dot{\boldsymbol{z}} + \mathsf{k}_{o_1}\boldsymbol{z} + \boldsymbol{t}_{o_1}$.

III. Deformable Object Manipulation

In this section we show how to determine the necessary end effector accelerations that will move the system along a desired direction while respecting constraints on the object's admissible deformation of the form:

$$\|\boldsymbol{z}_2\|_\infty \le \sigma \quad (9)$$

Using (6b), and with $\mathsf{m}_{o_{22}}$ invertible, we solve for $\ddot{\boldsymbol{z}}_2$:

$$\ddot{\boldsymbol{z}}_2 = -(\mathsf{m}_{o_{22}})^{-1}[(\mathsf{m}_{o_{12}})^T\ddot{\boldsymbol{z}}_1 + \boldsymbol{c}_{o_2} + \mathsf{d}_{o_2}\dot{\boldsymbol{z}} + \mathsf{k}_{o_2}\boldsymbol{z} + \boldsymbol{t}_{o_2}]$$

If we define now the following terms:

$$\tilde{\mathsf{m}}_{o_{11}}(\boldsymbol{z}) \triangleq \mathsf{m}_{o_{11}}(\boldsymbol{z}) - \mathsf{m}_{o_{12}}(\boldsymbol{z})\,[\mathsf{m}_{o_{22}}(\boldsymbol{z})]^{-1}\,[\mathsf{m}_{o_{12}}(\boldsymbol{z})]^T,$$
$$\tilde{\boldsymbol{c}}_{o_1}(\boldsymbol{z},\dot{\boldsymbol{z}}) \triangleq \boldsymbol{c}_{o_1}(\boldsymbol{z},\dot{\boldsymbol{z}}) - \mathsf{m}_{o_{12}}(\boldsymbol{z})\,[\mathsf{m}_{o_{22}}(\boldsymbol{z})]^{-1}\,\boldsymbol{c}_{o_2}(\boldsymbol{z},\dot{\boldsymbol{z}}),$$
$$\tilde{\mathsf{d}}_{o_1}(\boldsymbol{z}) \triangleq \mathsf{d}_{o_1} - \mathsf{m}_{o_{12}}(\boldsymbol{z})\,[\mathsf{m}_{o_{22}}(\boldsymbol{z})]^{-1}\,\mathsf{d}_{o_2}$$
$$\tilde{\mathsf{k}}_{o_1}(\boldsymbol{z}) \triangleq \mathsf{k}_{o_1} - \mathsf{m}_{o_{12}}(\boldsymbol{z})\,[\mathsf{m}_{o_{22}}(\boldsymbol{z})]^{-1}\,\mathsf{k}_{o_2},$$
$$\boldsymbol{t}_{o_1}(\boldsymbol{z}) \triangleq \boldsymbol{t}_{o_1}(\boldsymbol{z}) - \mathsf{m}_{o_{12}}(\boldsymbol{z})\,[\mathsf{m}_{o_{22}}(\boldsymbol{z})]^{-1}\,\boldsymbol{t}_{o_2}(\boldsymbol{z})$$

and apply to the object the feedback linearizing force:

$$\boldsymbol{F} = \tilde{\boldsymbol{c}}_{o_1} + \tilde{\mathsf{d}}_{o_1}\dot{\boldsymbol{z}} + \tilde{\mathsf{k}}_{o_1}\boldsymbol{z} + \tilde{\boldsymbol{t}}_{o_1} + \tilde{\mathsf{m}}_{o_{11}}\boldsymbol{u}_o, \quad (10)$$

equations (6a)-(6b) become:

$$\ddot{\boldsymbol{z}}_1 = \boldsymbol{u}_o \quad (11a)$$
$$\ddot{\boldsymbol{z}}_2 = -\mathsf{m}_{o_{22}}^{-1}[\mathsf{m}_{o_{12}}^T\ddot{\boldsymbol{z}}_1 + \boldsymbol{c}_{o_2} + \mathsf{d}_{o_2}\dot{\boldsymbol{z}} + \mathsf{k}_{o_2}\boldsymbol{z} + \boldsymbol{t}_{o_2}] \quad (11b)$$

Define the output of (11b) as $\boldsymbol{z}_1 - \boldsymbol{z}_{1d}$, where $\boldsymbol{z}_{1d}$ is the desired position of the grasp point. In velocity field tracking, $\dot{\boldsymbol{z}}_1 - \dot{\boldsymbol{z}}_{1d}$, and $\boldsymbol{z}_1 - \boldsymbol{z}_{1d} \equiv 0$. The zero dynamics of (11b) is

$$\mathsf{m}_{o_{22}}\ddot{\boldsymbol{z}}_2 = -\boldsymbol{c}_{o_2}\Big|_{\dot{\boldsymbol{z}}_1=\boldsymbol{0}} - \mathsf{d}_{o_{22}}\dot{\boldsymbol{z}}_2 - \mathsf{k}_{o_{22}}\boldsymbol{z}_2 - \mathsf{k}_{o_{21}}\boldsymbol{z}_{1d} - \boldsymbol{t}_{o_2}, \quad (12)$$

with $\mathsf{d}_{o_2} = \begin{bmatrix}\mathsf{d}_{o_{21}} & \mathsf{d}_{o_{22}}\end{bmatrix}$, and $\mathsf{k}_{o_2} = \begin{bmatrix}\mathsf{k}_{o_{21}} & \mathsf{k}_{o_{22}}\end{bmatrix}$. This system equilibrates at $\boldsymbol{z}_2^*$ given by $\mathsf{k}_{o_{22}}\boldsymbol{z}_2^* + \boldsymbol{t}_{o_2} + \mathsf{k}_{o_{21}}\boldsymbol{z}_{1d} = \boldsymbol{0}$. We can show that the zero dynamics are GAS:

Lemma III.1 *Equation* (11b)*, restricted in the set where* $\dot{\boldsymbol{z}}_1 = \boldsymbol{0}$*, is globally asymptotically stable around* $\boldsymbol{z}_2^*$ *defined by:* $\mathsf{k}_{o_2}\boldsymbol{z} + \boldsymbol{t}_{o_2} = \boldsymbol{0}$.

Proof: Consider the following storage function: $V \triangleq \frac{1}{2}\dot{\boldsymbol{z}}^T\mathsf{M}_o\dot{\boldsymbol{z}} + \frac{1}{2}\boldsymbol{z}^T\mathsf{K}_o\,\boldsymbol{z} + U$, where U is the potential energy of the object due to gravity. Differentiating V and restricting it on $\ddot{\boldsymbol{z}}_1 = \boldsymbol{u}_o$, $\ddot{\boldsymbol{z}}_1 = \dot{\boldsymbol{z}}_1 = 0$:

$$\dot{V} = (\dot{\boldsymbol{z}}_2)^T\mathsf{m}_{o_{22}}\,\ddot{\boldsymbol{z}}_2 + \frac{1}{2}(\dot{\boldsymbol{z}}_2)^T\dot{\mathsf{m}}_{o_{22}}\dot{\boldsymbol{z}}_2 + (\dot{\boldsymbol{z}}_2)^T\mathsf{k}_{o_2}\boldsymbol{z} + \boldsymbol{t}_{o_2}\dot{\boldsymbol{z}}_2.$$

With matrix $\dot{\mathsf{M}}_o - 2\mathsf{C}_o$ being skew-symmetric, the principal submatrix $\dot{\mathsf{m}}_{o_{22}} - 2\mathsf{c}_{o_{22}}$, is too. Using (12), $\dot{V} = -\dot{\boldsymbol{z}}_2^T\mathsf{d}_{o_{22}}\dot{\boldsymbol{z}}_2$, where $\mathsf{d}_{o_{22}}$ is positive definite. The internal dynamics system is strictly passive with respect to the output $\dot{\boldsymbol{z}}_2$ on the zero dynamics manifold, if $\dot{\boldsymbol{z}}_1 = 0$. In addition, $\dot{V} = 0 \Rightarrow \dot{\boldsymbol{z}}_2 = \boldsymbol{0} \overset{(6b)}{\Rightarrow} \boldsymbol{z}_2 = \boldsymbol{z}_2^*$, which means that the equilibrium point of the zero dynamics is globally asymptotically stable. ■

With $\boldsymbol{\eta} \triangleq \begin{bmatrix}(\boldsymbol{z}_2 - \boldsymbol{z}_2^*)^T & (\dot{\boldsymbol{z}}_2)^T\end{bmatrix}^T$, (6b) is rewritten:

$$\dot{\boldsymbol{\eta}} = \boldsymbol{\xi}(\boldsymbol{\eta},\boldsymbol{\nu}), \quad (13)$$

where, given that $\boldsymbol{z}_1 - \boldsymbol{z}_{1d} \equiv \boldsymbol{0}$,

$$\boldsymbol{\nu} \triangleq \begin{bmatrix}\boldsymbol{0} & (\dot{\boldsymbol{z}}_1)^T & (\ddot{\boldsymbol{z}}_1)^T\end{bmatrix}^T. \quad (14)$$

By Lemma III.1, (6b) is locally input-to-state stable [18]:

$$\|\boldsymbol{\eta}\|_\infty \le \beta(\|\boldsymbol{\eta}(\boldsymbol{0})\|_\infty, 0) + \gamma\left(\sup_{0\le\tau\le t}\|\boldsymbol{\nu}\|_\infty\right). \quad (15)$$

To obtain an estimate of the function γ, we linearize the zero dynamics near the origin $\boldsymbol{z}_2 = \boldsymbol{z}_2^* = 0$, $\dot{\boldsymbol{z}}_2 = 0$:

$$\dot{\boldsymbol{\eta}} = \mathsf{A}_u\boldsymbol{\eta} + \mathsf{B}_u\boldsymbol{\nu}, \quad (16)$$

where $\mathsf{A}_u = \frac{\partial\boldsymbol{\xi}}{\partial\boldsymbol{\eta}}\Big|_{\boldsymbol{\eta}=\boldsymbol{0},\boldsymbol{\nu}=\boldsymbol{0}}$, $\mathsf{B}_u = \frac{\partial\boldsymbol{\xi}}{\partial\boldsymbol{\nu}}\Big|_{\boldsymbol{\eta}=\boldsymbol{0},\boldsymbol{\nu}=\boldsymbol{0}}$. We will assume that $(\mathsf{A}_u, \mathsf{B}_u)$ is controllable pair.

Lemma III.2 *The matrix* A_u *of* (16) *has eigenvalues on the closed left half plane.*

Proof: By contradiction, using III.1, and assuming that A_u has eigenvalues with positive real parts. ■

If A_u is Hurwitz, a Lyapunov matrix is computed as: $\mathsf{P}(t)\ \mathsf{A}_u(t) + \mathsf{A}_u^T(t)\mathsf{P}(t) = -\mathsf{I}$. If A_u is not Hurwitz, given that $(\mathsf{A}_u, \mathsf{B}_u)$ is controllable, we design a control law $\boldsymbol{\nu} = \mathsf{H}\ \boldsymbol{\eta}$ with $\|\mathsf{H}\ \boldsymbol{\eta}\| \le \mu$ so that $(\mathsf{A}_u + \mathsf{B}_u\ \mathsf{H})$ is Hurwitz [19]. The Lyapunov matrix is then computed as: $\mathsf{P}(t)\ (\mathsf{A}_u + \mathsf{B}_u\ \mathsf{H}) + (\mathsf{A}_u + \mathsf{B}_u\ \mathsf{H})^T\mathsf{P}(t) = -\mathsf{I}$, and γ is then estimated as

$$\gamma(\rho) \triangleq 4\sqrt{2(n-m)^3}\lambda_M(\mathsf{P})\sqrt{\frac{\lambda_M(\mathsf{P})}{\lambda_m(\mathsf{P})}}\rho, \quad (17)$$

where $\lambda_M(\mathsf{P}), \lambda_m(\mathsf{P})$ are the maximum and minimum eigenvalue of $\mathsf{P}(t)$, respectively. Suppose the reference velocities are such that (14) is upper bounded by

$$\nu_{max} \triangleq \frac{\sigma - \sup\|\boldsymbol{z}_2^*\|_\infty}{8(n-m)^2\lambda_M(\mathsf{P})\,\lambda_M(\mathsf{B}_u)}\sqrt{\frac{\lambda_m(\mathsf{P})}{\lambda_M(\mathsf{P})}}, \quad (18)$$

where $\lambda_M(\mathsf{B}_u) = \sqrt{\lambda_{max}\mathsf{B}_u\mathsf{B}_u^T}$. Then, note that (15) yields $\limsup\|\boldsymbol{\eta}\|_\infty \leq \gamma(\sup\|\mathsf{B}_u\boldsymbol{\nu}\|)$. Given that $\boldsymbol{\eta} \triangleq [(\boldsymbol{z}_2 - \boldsymbol{z}_2^*)^T, \dot{\boldsymbol{z}}_2^T]^T \Rightarrow \|\boldsymbol{\eta}\|_\infty + \sup\|\boldsymbol{z}_2^*\|_\infty \geq \|\boldsymbol{z}_2\|_\infty$, we have $\|\boldsymbol{z}_2\|_\infty < \sigma$ if: $\|\boldsymbol{\eta}\|_\infty + \sup\|\boldsymbol{z}_2^*\|_\infty < \sigma \Leftrightarrow \|\boldsymbol{\eta}\|_\infty < \sigma - \sup\|\boldsymbol{z}_2^*\|_\infty$. Using (17) we see that the above holds if $\sup\|\boldsymbol{\nu}\|_\infty < \nu_{max}$. By putting an upper bound on the norm of the grasp point velocities, and by requiring this bound to be smaller than ν_{max}, the system does not move fast enough to excite unacceptable deformations on the object:

Proposition III.3 *Consider* (11a)-(13)*, and let* (16) *be the linearization of* (13) *in a region $\mathcal{N}$ of* $(\dot{\boldsymbol{z}}_1, \boldsymbol{\eta}) = (\mathbf{0}, \mathbf{0})$*. If* $(\mathsf{A}_u, \mathsf{B}_u)$ *is controllable,* $(\mathsf{A}_u{+}\mathsf{B}_u\ \mathsf{H})$ *with* $\|\mathsf{H}\boldsymbol{\eta}\| \leq \mu \quad \forall\, \boldsymbol{\eta} \in \mathcal{N}$ *is Hurwitz (if A_u is Hurwitz, μ can be set to zero), and the following inequality holds:*

$$\nu_{max} - \sup\|\dot{\boldsymbol{z}}_1\|_\infty - \mu \geq s > 0, \quad (19)$$

where ν_{max} is given by (18)*, then there exists a control law:*

$$\boldsymbol{u}_o = \mathsf{L}\dot{\boldsymbol{e}}_{z_1} = \mathsf{L}(\dot{\boldsymbol{z}}_1 - \dot{\boldsymbol{z}}_{1d}) \quad (20)$$

that ensures tracking of the reference end-effector velocity, $\dot{\boldsymbol{z}}_{1d}$, while $\|\boldsymbol{z}_2\|_\infty \leq \sigma$.

Proof: If A_u is Hurwitz, the solution of the Lyapunov equation provides $\mathsf{P}(t)$; γ, ν_{max} are computed from (17) and (18), respectively. Since (11b) is locally input-to-state stable, (17) implies:

$$\|\boldsymbol{\eta}\|_\infty \leq 4\sqrt{2(n-m)^3}\lambda_M(\mathsf{P})\sqrt{\frac{\lambda_M(\mathsf{P})}{\lambda_m(\mathsf{P})}}\|\mathsf{B}_u\,\boldsymbol{\nu}\|_\infty. \quad (21)$$

From the definition of $\boldsymbol{\eta} = [(\boldsymbol{z}_2 - \boldsymbol{z}_2^*)^T, (\dot{\boldsymbol{z}})_2^T]^T$, it follows $\|\boldsymbol{\eta}\|_\infty + \sup\|\boldsymbol{z}_2^*\|_\infty \geq \|\boldsymbol{z}_2\|_\infty$. This, in turns, implies $\|\boldsymbol{\eta}\|_\infty + \sup\|\boldsymbol{z}_2^*\|_\infty \leq \sigma \Rightarrow \|\boldsymbol{z}_2\|_\infty \leq \sigma$. Therefore, in order for $\|\boldsymbol{z}_2\|_\infty \leq \sigma$ it suffices that

$$\|\boldsymbol{\eta}\|_\infty \leq \sigma - \sup\|\boldsymbol{z}_2^*\|_\infty. \quad (22)$$

Equating the right hand sides of (21) and (22), we have

$$\sup\|\boldsymbol{\nu}\|_\infty \leq \frac{\sigma - \sup\|\boldsymbol{z}_2^*\|_\infty}{8(n-m)^2\lambda_M(\mathsf{P})\,\lambda_M(\mathsf{B}_u)}\sqrt{\frac{\lambda_m(\mathsf{P})}{\lambda_M(\mathsf{P})}}, \quad (23)$$

where $\lambda_M(\mathsf{B}_u)^2$ is the maximum eigenvalue of $\mathsf{B}_u^T\mathsf{B}_u$. Given $\boldsymbol{\nu} = \begin{bmatrix}(\dot{\boldsymbol{z}})_1^T & (\boldsymbol{u}_o)^T\end{bmatrix}^T$, we have: $\sup\|\boldsymbol{\nu}\|_\infty \leq \sup\|\dot{\boldsymbol{z}}_1\|_\infty + \sup\|\boldsymbol{u}_o\|$. From (23), follows $\sup\|\boldsymbol{u}_o\| \leq \nu_{max} - \sup\|\dot{\boldsymbol{z}}_1\|_\infty \Rightarrow \|\boldsymbol{z}_2\|_\infty \leq \sigma$. If $\nu_{max} - \sup\|\dot{\boldsymbol{z}}_1\|_\infty > s > 0$, we achieve $\|\boldsymbol{z}_2\|_\infty \leq \sigma$ by making $\sup\|\boldsymbol{u}_o\|_\infty \leq s$. For bounded $\dot{\boldsymbol{e}}_{z_1}(0)$, we can design [19] a semi-globally stabilizing control law $\|\mathsf{L}\dot{\boldsymbol{e}}_{z_1}\| < s$ which respects (9).

If A_u is not Hurwitz, then we design a control law $\boldsymbol{\nu} = \mathsf{H}\,\boldsymbol{\eta}$ so that $\|\mathsf{H}\,\boldsymbol{\eta}\| \leq \mu$ and $(\mathsf{A}_u{+}\mathsf{B}_u\ \mathsf{H})$ is Hurwitz. The conditions for the existence of such a control law are guaranteed by Lemma III.2. Through $\boldsymbol{\nu}$ we could stabilize (13):

$$\boldsymbol{\nu} = \mathsf{H}\,\boldsymbol{\eta} = \begin{bmatrix}\hat{\boldsymbol{e}}_{z_1}^T & \hat{\dot{\boldsymbol{z}}}_1^T & \hat{\boldsymbol{u}}_o^T\end{bmatrix}^T \quad (24)$$

But $\boldsymbol{\nu}$ is determined by (11a):

$$\boldsymbol{\nu} = \begin{bmatrix}\mathbf{0} & \dot{\boldsymbol{z}}_1^T & \boldsymbol{u}_o^T\end{bmatrix}^T \quad (25)$$

For (16), the difference between (24) and (25) is a disturbance $\delta\boldsymbol{\nu} = \begin{bmatrix}-\hat{\boldsymbol{e}}_{z_1}^T & (\dot{\boldsymbol{z}}_{1d} - \hat{\dot{\boldsymbol{z}}}_1)^T & (\boldsymbol{u}_o - \hat{\boldsymbol{u}}_o)^T\end{bmatrix}^T$. Then,

$$\sup\|\delta\boldsymbol{\nu}\|_\infty \leq \sup\|\dot{\boldsymbol{z}}_1\|_\infty + \mu + \sup\|\boldsymbol{u}_o\|, \quad (26)$$

and the solution of $\mathsf{P}(t)\ (\mathsf{A}_u{+}\mathsf{B}_u\ \mathsf{H}){+}(\mathsf{A}_u{+}\mathsf{B}_u\ \mathsf{H})^T\mathsf{P}(t) = -\mathsf{I}$ provides matrix $\mathsf{P}(t)$ for which:

$$\|\boldsymbol{\eta}\|_\infty \leq 4\sqrt{2(n-m)^3}\lambda_M(\mathsf{P}^o)\sqrt{\frac{\lambda_M(\mathsf{P})}{\lambda_m(\mathsf{P})}}\|\mathsf{B}_u\boldsymbol{\nu}\|_\infty.$$

For $\|\boldsymbol{z}_2\|_\infty \leq \sigma$, we should have: $\sup\|\delta\boldsymbol{\nu}\|_\infty \leq \nu_{max}$, and given that $\nu_{max} - \sup\|\dot{\boldsymbol{z}}_1\|_\infty - \mu \geq s > 0$, (26), gives $\sup\|\boldsymbol{u}_o\|_\infty \leq s$. Based on [19], we design a control law $\boldsymbol{u}_o = \mathsf{L}\dot{\boldsymbol{e}}_{z_1}$ that semiglobally stabilizes (11a), with $\|\,\mathsf{L}\dot{\boldsymbol{e}}_{z_1}\| < s$. ■

IV. Robot Force Control

To realize the desired acceleration input, $\mathsf{L}\dot{\boldsymbol{e}}_{z_1}$, we close a force feedback loop around our current velocity feedback. If $\tilde{\boldsymbol{f}}$ is the force exerted on the object, the acceleration error will be $\Delta\boldsymbol{u}_o = (\tilde{\mathsf{m}}_{o_{11}})^{-1}(\tilde{\boldsymbol{f}} - \boldsymbol{f})$. The end-effector dynamics are:

$$\ddot{\boldsymbol{z}}_1 = \mathsf{L}\dot{\boldsymbol{e}}_{z_1} + \Delta\boldsymbol{u}_o. \quad (27)$$

Considering (8), we see that the task space control input:

$$\mathcal{T} = [\mathcal{M} + \mathsf{m}_{o_{11}} - \mathsf{m}_{o_{12}}(\mathsf{m}_{o_{22}})^{-1}\mathsf{m}_{o_{12}}](\boldsymbol{w} - \boldsymbol{N}) \quad (28)$$

feedback linearizes the actuated task space dynamics $\ddot{\boldsymbol{z}}_1 \equiv \ddot{\boldsymbol{x}}_a = \boldsymbol{w}$. The new input, $\boldsymbol{w}$ will now be defined as:

$$\boldsymbol{w} = \mathsf{L}\dot{\boldsymbol{e}}_{z_1} - k_1\Delta\boldsymbol{u}_o - k_2\int_0^t \Delta\boldsymbol{u}_o \mathrm{d}s, \quad (29)$$

where $k_1,\ k_2 > 0$ are control gains. Substituting for $\boldsymbol{w}$ using (29) in (28) and $\mathcal{T}$ of (28) in (8), $\Delta\ddot{\boldsymbol{x}}_a = -k_1\Delta\boldsymbol{u}_o - k_2\int_0^t \Delta\boldsymbol{u}_o\mathrm{d}s$, where

$$\Delta\ddot{\boldsymbol{x}}_a \triangleq \ddot{\boldsymbol{x}}_a - \mathsf{L}\dot{\boldsymbol{e}}_{z_1} = \ddot{\boldsymbol{z}}_1 - \mathsf{L}\dot{\boldsymbol{e}}_{z_1}. \quad (30)$$

Remark IV.1 *In view of* (29)*, one can enforce the bounded task velocity condition* (19)*, by scaling the gain matrix* L *and gains* k_1*,* k_2 *by a function of the type* $1 - \tanh(\nu_{max} - \mu - \sup\|\dot{\boldsymbol{z}}_1\|_\infty)$.

A. Task Space Potential Field Velocity Tracking

The desired velocity at each point in the task space is given as $\dot{\boldsymbol{z}}_{1d} = -k\nabla\varphi(\boldsymbol{x}_a)$, with $k > 0$ a constant. The condition for stabilizability of Proposition III.3, (19), follows from the saturated linear input construction of [19]. Parameter s in (19) is the upper bound of the allowable task space acceleration input, $\mathsf{L}\dot{\boldsymbol{e}}_{z_1} < \nu_{max} - \sup\|\dot{\boldsymbol{z}}_1\|_\infty - \mu$. From (19), $\|\mathsf{L}\dot{\boldsymbol{e}}_{z_1}\| \leq \|\mathsf{L}\|\,\|\dot{\boldsymbol{e}}_{z_1}\| = \|\mathsf{L}\|\ \ \|\dot{\boldsymbol{z}}_1 - \dot{\boldsymbol{z}}_{1d}\| \leq \|\mathsf{L}\|\ \ (\|\dot{\boldsymbol{z}}_1\| +$

$\|\dot{\boldsymbol{z}}_{1d}\|) \leq \|\mathsf{L}\| \ (\sup \|\dot{\boldsymbol{z}}_1\|_\infty + k\|\nabla\varphi\|)$. Thus the constraint $\mathsf{L}e_y^o < v_s - h^o - \mu$ is respected if

$$k\|\nabla\varphi\| < \left(v_s - \mu - (1+\|\mathsf{L}\|)h^o\right)\|\mathsf{L}\|^{-1}. \qquad (31)$$

There are two ways to satisfy inequality (31) [19]: either by decreasing k or by decreasing ε.

B. Redundancy Resolution

Realizing (28) through $\boldsymbol{T}_r$ requires resolution of the robot's kinematic redundancy at the *dynamic* level. It is well known that Jacobian pseudoinversion inevitably [16] generates instabilities [20]. We resolve the kinematic redundancy by assigning the desired accelerations to the mobile base and the manipulator, separately. Given (1), we define the projection matrices S_b and S_a so that $\mathrm{range}[\mathsf{S}_b] = \mathrm{range}[\mathsf{J}_{A_b}^T]$, and $\mathrm{range}[\mathsf{S}_a] = \mathrm{kernel}[\mathsf{J}_{A_b}] = \mathrm{range}[\mathsf{J}_{A_b}^T]^\perp$. The desired accelerations for the base and the manipulator will then be:

$$\ddot{\boldsymbol{q}}_{bd} = \mathsf{S}_b\boldsymbol{w} + k_3(\dot{\boldsymbol{q}}_b + k\mathsf{S}_b\nabla\varphi),$$
$$\ddot{\boldsymbol{q}}_{ad} = (\mathsf{J}_A\mathsf{S}_a)^{-1}\left(\boldsymbol{w} - \dot{\mathsf{J}}_A\mathsf{S}_a\dot{\boldsymbol{q}}_a\right),$$

where k_3 is a positive control gain. Substituting $\ddot{\boldsymbol{q}}_{bd}$ and $\ddot{\boldsymbol{q}}_{ad}$ for $\ddot{\boldsymbol{q}}_b$ and $\ddot{\boldsymbol{q}}_a$ in (7), yields the required joint-space control.

V. Stability of the Closed Loop System

Differentiating (30) with respect to time,

$$\frac{1}{k_2}\Delta\dot{\boldsymbol{u}}_o = -\frac{1}{k_1}\Delta\boldsymbol{u}_o - \frac{1}{k_1k_2}(\Delta\boldsymbol{x}_a)^{(3)}, \qquad (32)$$

where $(\Delta\boldsymbol{x}_a)^{(3)}$ is the third-order time derivative of $\Delta\boldsymbol{x}_a$. Letting $\ddot{\boldsymbol{z}}_{1d} = 0$, (27) can be combined with (32) as follows:

$$\ddot{\boldsymbol{e}}_{z_1} = \mathsf{L}\,\dot{\boldsymbol{e}}_{z_1} + \Delta\boldsymbol{u}_o \qquad (33a)$$
$$\epsilon\,\Delta\dot{\boldsymbol{u}}_o = -\frac{1}{k_1}\Delta\boldsymbol{u}_o - \frac{\epsilon}{k_1}\Delta\boldsymbol{x}_a^{(3)} \qquad (33b)$$

where k_2 is chosen so that $\epsilon \triangleq \frac{1}{k_2}$ is very small. Comparing (30) with (27) after differentiating both with respect to time, we have $(\Delta\boldsymbol{x}_a)^{(3)} = \Delta\dot{\boldsymbol{u}}_o$. Then, (33b) becomes

$$\epsilon\Delta\dot{\boldsymbol{u}}_o = -\frac{1}{k_1+1}\Delta\boldsymbol{u}_o \qquad (34)$$

Proposition V.1 (System Stability) *Consider the system* (33a) – (34) *and let* P_e *be the solution of the Lyapunov equation for* (33a). *If* $k_2 > k_2^* \triangleq \lambda_M(\mathsf{P}_e)^2$, *where* $\lambda_M(\mathsf{P}_e)$ *is the maximum eigenvalue of* P_e, *then the origin of the system* (33a) – (34) *is exponentially stable.*

Proof: Setting $\epsilon = 0$ in (34) and substituting in (33a):

$$\ddot{\boldsymbol{e}}_{z_1} = \mathsf{L}\,\dot{\boldsymbol{e}}_{z_1} \qquad (35)$$

We can compute a Lyapunov function for (35): $W_1(\dot{\boldsymbol{e}}_{z_1}) = (\dot{\boldsymbol{e}}_{z_1})^T\mathsf{P}_e\ \dot{\boldsymbol{e}}_{z_1}$ Setting $\tau = \frac{t-t_0}{\epsilon}$ and $\epsilon = 0$ in (34) yields: $\frac{\mathrm{d}\Delta\boldsymbol{u}_o}{\mathrm{d}\tau} = -\frac{1}{k_1+1}\Delta\boldsymbol{u}_o$, and with $\mathsf{P}_u = \frac{k_1+1}{2}\mathsf{I}$, a Lyapunov function for this system is defined: $W_2(\Delta\boldsymbol{u}_o) = (\Delta\boldsymbol{u}_o)^T\mathsf{P}_u\ \Delta\boldsymbol{u}_o$. For (33a)-(34), the Lyapunov function candidate $W_3(\dot{\boldsymbol{e}}_{z_1}, \Delta\boldsymbol{u}_o) \triangleq W_1(\dot{\boldsymbol{e}}_{z_1}) + W_2(\Delta\boldsymbol{u}_o)$ yields

$$\dot{W}_3 = -\|\dot{\boldsymbol{e}}_{z_1}\|^2 - k_2\|\Delta\boldsymbol{u}_o\|^2 + 2(\dot{\boldsymbol{e}}_{z_1})^T\mathsf{P}_e\ \Delta\boldsymbol{u}_o$$
$$\leq -\|\dot{\boldsymbol{e}}_{z_1}\|^2 - k_2\|\Delta\boldsymbol{u}_o\|^2 + 2\lambda_M(\mathsf{P}_e)\|\dot{\boldsymbol{e}}_{z_1}\|\ \|\Delta\boldsymbol{u}_o\|.$$

For $k_2 > \lambda_M(\mathsf{P}_e)^2$, the above reduces to: $\dot{W}_3 \leq -(\|\dot{\boldsymbol{e}}_{z_1}\| - \|\Delta\boldsymbol{u}_o\|)^2 - \left(1 - \frac{\lambda_M(\mathsf{P}_u)^2}{k_2}\right)\|\dot{\boldsymbol{e}}_{z_1}\|^2 < 0$ for all $\dot{\boldsymbol{e}}_{z_1}, \Delta\boldsymbol{u}_o \neq \boldsymbol{0}$. ■

VI. Simulations

Consider a nonholonomic mobile manipulator carrying a suspended beam (Fig. 1). We want to move the beam from $(x, y, \theta, q_1, q_2, \phi) = (-8.5, 5.5, 0, \frac{\pi}{3}, -\frac{\pi}{2}, 0)$ to $(0, 0, 0, \frac{\pi}{2}, -\frac{\pi}{2}, 0)$ with a bounded swing $|\phi| \leq \frac{\pi}{6}$. The motion of the end-effector is nonholonomic, because the arm cannot rotate around the vertical axis. The velocity field is

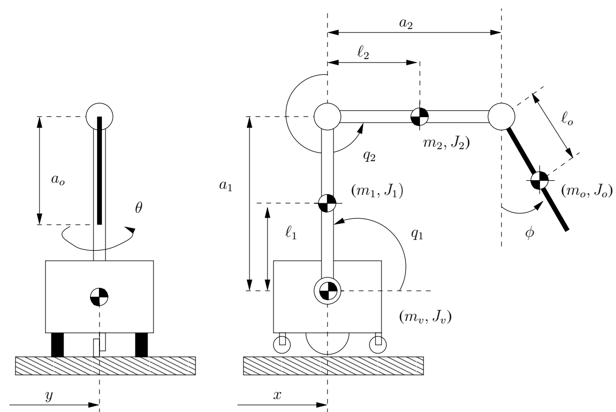

Fig. 1. The mobile manipulator model used in simulations.

generated by the dipolar potential function [21]: $\varphi(\boldsymbol{x}_a) = \frac{p_x^2+p_y^2}{[p_x^2+p_y^2]^2+p_x^2]^{1/2}} + (p_z-1)^2$. Assuming an internal damping coefficient $d = 1$, parameter ν_{max} is $1.089 \cdot 10^{-3}$. With $\sup\|\boldsymbol{z}_1\|_\infty = \frac{\nu_{max}}{2}$, we choose $\varepsilon = 1.089 \cdot 10^{-4}$. To illustrate the robustness of the approach to parameter uncertainty in the object model, in the simulations we used an internal damping coefficient of $d = 0.1$ instead, and we increased ε by an order of magnitude. We simulated noise as a high frequency force disturbance $0.005\sin t$, and parameter uncertainty in the robot model as a force bias, $0.05[N]$. Figure 5 depicts the evolution of the (simulated) force error, $\Delta\boldsymbol{u}_o$. Figure 2 shows the evolution of the configuration of the system over time. The swing angle of the suspended beam is given separately in Figure 3, from which it can be verified that the observed deformations are below the admissible limit. Figure 4 shows the evolution with time of the task space position errors, indicating asymptotic convergence to zero.

VII. Conclusions

We developed a velocity field tracking control scheme with PI force feedback, which enables the transport of deformable objects without them exhibiting excessive deformations. Velocity field tracking allows the methodology to be applicable to nonholonomic systems and providing the possibility for extensions to obstacle avoidance and navigation.

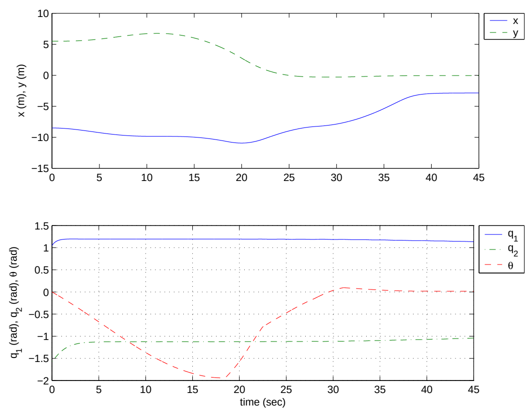

Fig. 2. Evolution of the system's state starting at q_0.

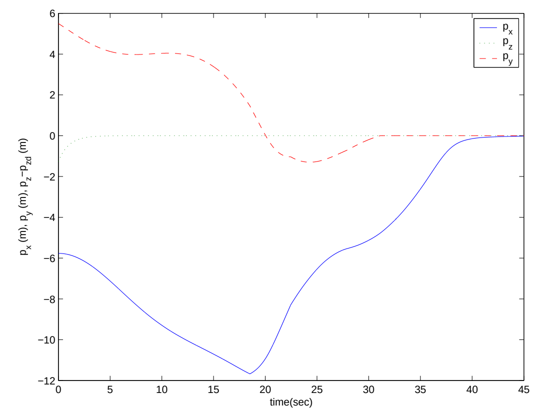

Fig. 4. End-effector position errors, with the system starting at q_0.

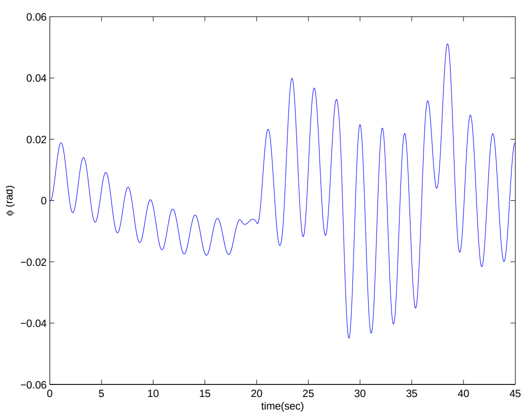

Fig. 3. Beam swing angle with the system starting at q_0.

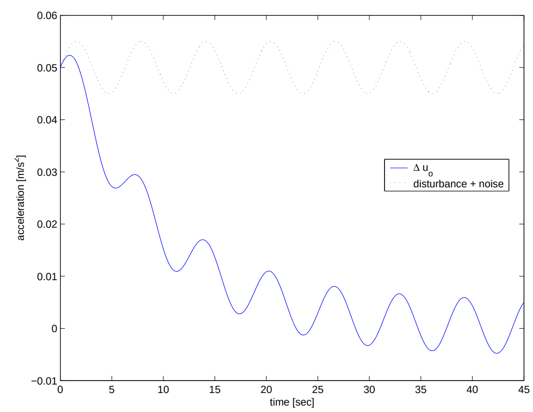

Fig. 5. Disturbance and noise suppression through PI force feedback.

REFERENCES

[1] K. Kosuge, M. Sakai, K. Kanitani, H. Yoshida, and T. Fukuda, "Manipulation of a flexible object by dual manipulators," in *IEEE Int. Conf. Robot. Autom.*, 1995, pp. 318–322.

[2] T. Yukawa, M. M. Uchiyama, and H. Inooka, "Cooperative control of a vibrating flexible object by a rigid dual-arm robot," in *IEEE Int. Conf. Robot. Autom.*, 1995, pp. 1820–1826.

[3] D. Sun, J. Mills, and Y. Liu, "Hybrid position and force control of two industrial robots manipulating a flexible sheet: Theory and experiment," in *IEEE Int. Conf. Robot. Autom.*, Leuven, Belgium, May 1998, pp. 1835–1840.

[4] W. K. Jr. and B. J. McCarragher, "Force fields in the manipulation of flexible materials," in *Proc. IEEE Int. Conf. Robot. Autom.*, Minneapolis, MN, April 1996, pp. 2352–2357.

[5] G. P. Starr, "Swing-free transport of suspended objects with a path-controlled robot manipulator," *ASME Journal of Dynamic Systems, Measurement and Control*, vol. 97, no. 1, pp. 97–100, March 1985.

[6] M. N. Sahinkaya, "Input shaping for vibration-free positioning of flexible systems," *Journal of Systems and Control Engineering*, vol. 205, no. I5, pp. 467–481, 2001.

[7] J. Wu, Z. Luo, K. Yamakita, and K. Ito, "Adaptive hybrid control of manipulators on uncertain flexible objects," *Advanced Robotics*, vol. 10, no. 5, pp. 469–485, 1996.

[8] Y. Liu and D. Sun, "Stabilizing a flexible beam handled by two manipulators via pd feedback," *IEEE Trans. Automat. Contr.*, vol. 45, no. 11, pp. 2159–2164, November 2000.

[9] A. Schlechter and D. Henrich, "Manipulating deformable linear objects: Manipulation skill for active damping of oscillations," in *IEEE/RSJ Int. Conf. Intell. Robot. Syst.*, Lausanne, Switzerland, September 2002, pp. 841–846.

[10] F. Abergg, D. Henrich, and H. Wörn, "Manipulationg deformable linear objects – vision based recognition of contact state transitions," in *Proceedings of the IEEE International Conference on Advanced Robotics*, Tokyo, October 1999, pp. 135–140.

[11] Y. Luo and B. Nelson, "Fusing force and vision feedbacks for manipulating deformable objects," *Journal of Robotic Systems*, vol. 18, no. 3, pp. 103–117, 2001.

[12] H. G. Tanner, S. G. Loizou, and K. J. Kyriakopoulos, "Nonholonomic navigation and control of multiple mobile manipulators," *IEEE Trans. Robot. Automat.*, vol. 19, no. 1, pp. 53–64, February 2003.

[13] P. Y. Li and R. Horowitz, "Passive velocity field control of mechanical manipulators," *IEEE Trans. Robot. Automat.*, vol. 15, no. 4, pp. 751–763, August 1999.

[14] E. Rimon and D. Koditschek, "Exact robot navigation using artificial potential functions," *IEEE Transactions on Robotics and Automation*, vol. 8, no. 5, pp. 501–518, October 1992.

[15] J. M. Hollerbach and K. C. Suh, "Redundancy resolution of manipulators through torque optimization," *IEEE J. Robot. Automat.*, vol. RA-3, no. 4, pp. 308–316, August 1987.

[16] K. O'Neil, "Divergence of linear acceleration-based redundancy resolution schemes," *IEEE Trans. Robot. Automat.*, vol. 18, no. 4, pp. 625–631, August 2002.

[17] H. Tanner and K. Kyriakopoulos, "A manipulated deformable object as an underactuated mechanical system," in *Robot Manipulation of Deformable Objects*, D. Henrich and H. Wörn, Ed. Springer, 2000, pp. 175–198.

[18] E. D. Sontag and Y. Wang, "New characterizations of input to state stability," *IEEE Trans. Automat. Contr.*, vol. 41, no. 9, pp. 1283–1294, September 1996.

[19] J. Alvarez-Ramírez, R. Suaréz, and J. Alvarez, "Semiglobal stabilization of multi-input linear systems with saturated linear state feedback," *Systems and Control Letters*, vol. 23, pp. 247–254, 1994.

[20] J. Hollerbach, "Redundancy resolution of manipulators through torque optimization," *IEEE J. Robot. Automat.*, vol. RA-3, no. 4, pp. 308–316, 1986.

[21] H. Tanner, S. Loizou, and K. Kyriakopoulos, "Nonholonomic stabilization with collision avoidance for mobile robots," in *IEEE/RSJ Int. Conf. Intell. Robot. Syst.*, Maui, Hawaii, October 2001, pp. 1220–1225.